International Journal of Control, Automation and Systems 19(1) (2021) 372-381
http://dx.doi.org/10.1007/s12555-019-0927-2
ISSN:1598-6446 eISSN:2005-4092
http://www.springer.com/12555

Neural Approximation-based Model Predictive Tracking Control of Non-holonomic Wheel-legged Robots

Jiehao Li, Junzheng Wang, Shoukun Wang, Wen Qi, Longbin Zhang, Yingbai Hu, and Hang Su*

Abstract: This paper proposes a neural approximation based model predictive control approach for tracking control of a nonholonomic wheel-legged robot in complex environments, which features mechanical model uncertainty and unknown disturbances. In order to guarantee the tracking performance of wheel-legged robots in an uncertain environment, effective approaches for reliable tracking control should be investigated with the consideration of the disturbances, including internal-robot friction and external physical interactions in the robot's dynamical system. In this paper, a radial basis function neural network (RBFNN) approximation based model predictive controller (NMPC) is designed and employed to improve the tracking performance for nonholonomic wheel-legged robots. Some demonstrations using a BIT-NAZA robot are performed to illustrate the performance of the proposed hybrid control strategy. The results indicate that the proposed methodology can achieve promising tracking performance in terms of accuracy and stability.

Keywords: Model predictive control, neural approximation, nonholonomic system, tracking control, wheel-legged robot.

1. INTRODUCTION

In the past few years, wheel-legged robots [1–3] have become widespread among applications that can operate in various uncertain or unreachable terrains, such as narrow space in damaged buildings after disasters, radiation environments, and complex working field. In the development and control of the wheel-legged robots, research interests have been attracted, and promising results have been achieved. For instance, the developed quadruped robot AZ-IMUT in [4] was capable of switching the control modes between legs and wheel tracking. A deformable wheeled robot based on origami structure was introduced in [5], and the robot can move quickly with large wheels and small gaps. A mechanically decoupled wheel-legged hybrid transformable robot, namely HyTRo-I in [6], was able to achieve the transformation between wheeled and legged configuration with improved shifting stability and a small number of transition steps. However, most of these wheel-legged robots are created with series mechanism, which is small in size and weak in payload and cannot meet the practical requirements in extreme situations such as disaster relief, combat platforms, and resource exploration. In order to meet the various terrains requirements, such as movement efficiency, velocity, stability, obstacle-negotiation, and improved payload capacity [7, 8], a new mobility structure that can transform between wheel and leg is proposed in this paper. However, its tracking control accuracy is affected due to its mechanical model uncertainty and unknown disturbances in complex environments under heavy loads. Few works have solved these challenges. Hence, this paper focuses on the tracking control of the developed novel electric parallel wheel-legged robot with payload capacity.

Accurate path tracking is one of the main challenges of autonomous mobile robots, and it has attracted many research interests in practical engineering fields. For example, the lateral control of four-wheel electric vehicles based on a delay linear quadratic regulator (LQR) control algorithm was proposed in [9]. In [10], a model-free adaptive sliding mode control (ASMC) was applied to the automatic parking system, and a dynamic compensator was introduced to solve the influence of integral saturation. In [11], a state observer enhanced sliding mode control

Manuscript received October 31, 2019; revised March 14, 2020; accepted April 18, 2020. Recommended by Editor Fumitoshi Matsuno. This study was supported by the Nation Natural Science Foundation of China under Grant 61773060, and China Scholarship Council under Grant 201906030066.

Jiehao Li, Junzheng Wang, and Shoukun Wang are with the State Key Laboratory of Intelligent Control and Decision of Complex Systems, Beijing Institute of Technology, Beijing, 100081, China (e-mails: {jiehao.li, wangjz, bitwsk}@bit.edu.cn). Wen Qi and Hang Su are with the Department of Electronics, Information and Bioengineering, Politecnico di Milano, 20133, Milan, Italy (e-mails: {hang.su, wen.qi}@polimi.it). Longbin Zhang is with the BioMEx Center and KTH Mechanics, KTH Royal Institute of Technology, SE-100 44 Stockholm, Sweden (e-mail: longbin@kth.se). Yingbai Hu is with the Department of Informatics, Technical University of Munich, Munich, 85748, Germany (e-mail: yingbai.hu@tum.de).
* Corresponding author.

(SMC) was implemented to an underwater robot system combined with unknown disturbances and uncertain nonlinearities. Besides, a vision-based model prediction control (MPC) was developed to guarantee a wheel mobile robot to follow the desired target in the polar coordinate [12]. For redundancy optimization in manipulators, a deep convolutional neural network (DCNN) structure was presented in [13].

However, one of these drawbacks of the methods mentioned above is that they do not explicitly consider the mechanical uncertainties and external dynamic interactions such as mechanical parameter variation, load transfer, and friction impact, which may lead to instability and inaccuracy in the tracking control [14, 15]. In practical systems, due to the existence of nonlinearities and uncertainties, accurate knowledge of the developed system model cannot be assumed.

In related works, task-space tracking based on fuzzy adaptive control (FAC) schemes for compensating the external disturbances and dynamics uncertainties are studied [16, 17]. Moreover, the nonlinear model predictive control scheme to track the desired trajectory based on neural-dynamic optimization is proposed [18]. Besides, for the robot vision system, a fast and robust deep convolutional neural networks are presented [19,20]. In this paper, a neural approximation-based model predictive tracking control of nonholonomic wheel-legged robots under uncertain disturbances is considered. The main contributions of the paper are summarized as follows:

- A novel wheel-legged robot with parallel mechanism is presented to improve the maneuverability and flexibility effectively.
- A neural approximation-based model predictive tracking controller is applied to eliminate the uncertain dynamics and external disturbances for the application of mobile robots, such as mechanical parameter variation and dynamic load disturbance.

The structure of this paper is organized as follows: Section 2 presents the problem formulation and the developed novel wheel-legged robot. In Section 3, the RBFNN approximation-based model predictive tracking control is introduced to achieve accurate tracking under uncertain internal and external disturbances. In Section 4, the system description of the developed electric parallel platform is introduced. Experimental results are presented to show the controller performance in Section 5, and a conclusion is drawn in Section 6.

2. PROBLEM FORMULATION

The formulation of the nonholonomic constraints for the wheel-legged robot can be addressed as

$$\dot{x}_c \sin\varphi_c - \dot{y}_c \cos\varphi_c = 0, \tag{1}$$

where (x_c, y_c) denote the centroid coordinate position of X-axis and Y-axis, respectively, and φ_c represents the corresponding heading angle.

Assuming that $q_{3\times1} = [x_c, y_c, \varphi_c]^T$ and $\mathcal{J}(q) = [\sin\varphi_c, -\cos\varphi_c, 0]$, the constraints formulation can be described as below:

$$\mathcal{J}(q)\dot{q} = 0. \tag{2}$$

Thus, the kinematic model of wheel-legged robot can be represented as

$$\begin{bmatrix} \dot{x}_c \\ \dot{y}_c \\ \dot{\varphi}_c \end{bmatrix} = \begin{bmatrix} \cos\varphi_c & 0 \\ \sin\varphi_c & 0 \\ 0 & 1 \end{bmatrix} \begin{bmatrix} v_c \\ \omega_c \end{bmatrix}, \tag{3}$$

where v_c denotes the robotic linear velocity of centroid; φ_c is the course angle, and ω_c represents the yaw rate.

Besides, considering the uncertainties and external dynamics, the wheel-legged robot of nonholonomic constraint model according to the Euler-Lagrangain can be described as

$$M(q)\ddot{q} + C(q,\dot{q})\dot{q} + G(q) = \mathcal{J}^T(q)(\lambda - F_d), \tag{4}$$

where $M(q) \in R^{n\times n}$ is the symmetric positive definite inertia matrix; $q \in R^n$ denotes the generalized coordinate; $C(q,\dot{q}) \in R^{n\times n}$ is the centripetal and Coriolis matrix; $G(q) \in R^n$ is the gravitational vector; $F_d \in R^{n\times n}$ is the mechanical uncertainties such as the friction of electric cylinder and spring force and external dynamics e.g. rolling resistance and road friction; $\lambda \in R^n$ represents the driving torque.

Position space decomposition by separating the control variables into position and attitude is an efficient solution for the control of the 6-DOF electric parallel platform. In general, the reference coordinate is set as $O_B - X_B Y_B Z_B$ while $O_U - X_U Y_U Z_U$ is set as the moving coordinate. The combination of the base and six servo motors are B_i (i = 1, 2, ..,6), and the coordinates in the moving coordinate system are U_i (i = 1, 2, ..., 6). Define θ_x, θ_y, θ_z are the rotation angle of X-axle, Y-axle and Z-axle, respectively. Δx, Δy, Δz are the corresponding displacement. Then, we have

$$\mathbf{P_B} = \mathbf{T}\mathbf{P_U} + \mathbf{U_0} + \mathbf{P_m}, \tag{5}$$

where $\mathbf{T}$ is the coordinate transformation matrix; $\mathbf{P_U}$ and $\mathbf{P_B}$ are the dynamic coordinate and static coordinate, respectively; $\mathbf{P_m} = [\Delta_x, \Delta_y, \Delta_z]^T$ and $\mathbf{U}_0 = [x, y, z]^T$.

Then the translation equation of can be described as

$$\begin{bmatrix} x_B \\ y_B \\ z_B \end{bmatrix} = \begin{bmatrix} x_U + \Delta_x + x \\ y_U + \Delta_y + y \\ z_U + \Delta_z + z \end{bmatrix} = \begin{bmatrix} x_U \\ y_U \\ z_U \end{bmatrix} + \mathbf{U}_0 + \mathbf{P_m}. \tag{6}$$

When the moving coordinate rotates around the X-axis, we can obtain

$$\begin{bmatrix} x_B \\ y_B \\ z_B \end{bmatrix} = \begin{bmatrix} x_U \\ y_U C\theta_x - z_U S\theta_x \\ y_U S\theta_x + z_U C\theta_x \end{bmatrix} = \mathbf{T_x} \begin{bmatrix} x_U \\ y_U \\ z_U \end{bmatrix}, \tag{7}$$

subjected to

$$\mathbf{T_x} = \begin{bmatrix} 1 & 0 & 0 \\ 0 & C\theta_x & -S\theta_x \\ 0 & S\theta_x & C\theta_x \end{bmatrix}. \tag{8}$$

Similarly, we can obtain the relationship of Y-axis and Z-axis as follows:

$$\begin{bmatrix} x_B \\ y_B \\ z_B \end{bmatrix} = \begin{bmatrix} x_U C\theta_y + z_U S\theta_y \\ y_U \\ -x_U S\theta_y + z_U C\theta_y \end{bmatrix} = \mathbf{T_y} \begin{bmatrix} x_U \\ y_U \\ z_U \end{bmatrix}, \tag{9}$$

$$\begin{bmatrix} x_B \\ y_B \\ z_B \end{bmatrix} = \begin{bmatrix} x_U C\theta_z - y_U S\theta_z \\ x_U S\theta_z + y_U C\theta_z \\ z_U \end{bmatrix} = \mathbf{T_z} \begin{bmatrix} x_U \\ y_U \\ z_U \end{bmatrix}, \tag{10}$$

subjected to

$$\mathbf{T_y} = \begin{bmatrix} C\theta_y & 0 & S\theta_y \\ 0 & 1 & 0 \\ -S\theta_y & 0 & C\theta_y \end{bmatrix}, \tag{11}$$

and

$$\mathbf{T_z} = \begin{bmatrix} C\theta_z & -S\theta_z & 0 \\ S\theta_z & C\theta_z & 0 \\ 0 & 0 & 1 \end{bmatrix}, \tag{12}$$

where ($C\theta_x$, $C\theta_y$, $C\theta_z$) denote ($\cos\theta_x$, $\cos\theta_y$, $\cos\theta_z$), respectively. ($S\theta_x$, $S\theta_y$, $S\theta_z$) represent ($\sin\theta_x$, $\sin\theta_y$, $\sin\theta_z$), respectively.

Property 1: The order of rotation can be defined as: X $\rightarrow$ Y $\rightarrow$ Z, in other words, rotating $\theta_x \rightarrow \theta_y \rightarrow \theta_z$, and then translating $\Delta x \rightarrow \Delta x \rightarrow \Delta x$.

Therefore, the position transformation matrix can be described as

$$\begin{bmatrix} x_B \\ y_B \\ z_B \end{bmatrix} = \mathbf{T}_x\mathbf{T_y}\mathbf{T}_z \begin{bmatrix} x_U \\ y_U \\ z_U \end{bmatrix} = \mathbf{T} \begin{bmatrix} x_U \\ y_U \\ z_U \end{bmatrix} + \mathbf{U}_0 + \mathbf{P_m}, \tag{13}$$

subjected to

$$\mathbf{T} = \begin{bmatrix} C_yC_z & -C_yS_z & S_y \\ S_xS_yC_z + C_xS_z & -S_xS_yS_z + C_xC_z & -S_xC_y \\ -C_xS_yC_z + S_xS_z & C_xS_yS_z + S_xC_z & C_xC_y \end{bmatrix}, \tag{14}$$

where S_x, S_y, S_z, C_x, C_y and C_z represent $\sin\theta_x$, $\sin\theta_y$, $\sin\theta_z$ $\cos\theta_x$, $\cos\theta_y$ and $\cos\theta_z$, respectively.

Through the position control of each electric cylinder, different attitudes of the robot can be realized. The offset of each electric cylinder can be addressed as follows:

$$\Delta L_i = \sqrt{(u_{ix}-B_{ix})^2+(u_{iy}-B_{iy})^2+(u_{iz}-B_{iz})^2} - L_i. \tag{15}$$

On the other hand, we assume that the trajectory of the robot is generated by the following reference system:

$$\begin{aligned} \dot{x}_r &= v_r \cos\varphi_r, \\ \dot{y}_r &= v_r \sin\varphi_r, \\ \dot{\varphi}_r &= \omega_r, \end{aligned} \tag{16}$$

where $q_r = [x_r, y_r, \varphi_r]^T$ is the reference state; (v_r, ω_r) is the reference velocity and yaw rate, respectively.

Property 2: The reference signals $(v_r, \omega_r \dot{v}_r, \dot{\omega}_r)$ is bounded, and satisfy with the as follows:

$$\int_t^{t+T} (|v_r(s)| + |\omega_r(s)|)\, ds \geq \mu, \tag{17}$$

where $T, \mu > 0$ and $\forall t \geq 0$.

Thus, the tracking problem with uncertain dynamics and external disturbances in this paper is equivalent to design the control law for the nonholonomic constraint system such that:

$$\lim_{t\to\infty} (q(t) - q_r(t)) = 0. \tag{18}$$

3. CONTROLLER DEVELOPMENT

3.1. Neural approximation

Uncertainties in practical robot systems can be divided into two parts, including internal interference and external dynamics, as shown in Fig. 1. The former mainly involves the case where the parameters such as mass and rotational inertia of the system are unknown. At the same time, the latter mainly refers to some unmodeled dynamics such as external disturbance and friction. For the developed wheel-legged robot, however, model uncertainties and external disturbances, such as mechanical parameter variation, external load disturbance, and unstructured uncertainty, do exist in the dynamics of the robot systems for tracking control.

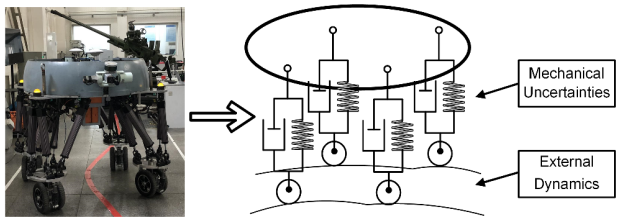

Fig. 1. Uncertain physical interaction in robot system.

To solve this problem, a RBFNN-based control approach is implemented to the robot system to deal with bounded disturbances and unmodeled dynamics. With the approximation capability of the RBFNN [21,22], a continuous smooth function $k(\mathrm{Z}): R^q \to R$ is defined, and then the RBFNN is used to estimate the uncertain dynamics and external disturbances.

$$k_{nn}(Z_{in}) = W^T S(Z_{in}), \tag{19}$$

where $Z_{in} \in \Omega \subset R^q$ denotes the input of RBFNN; $W = [w_1, w_2, \cdots, w_m] \in R^m$ represents the NN weight, and $m > 0$ is the NN node number in the hidden layer; $\mathcal{S}(Z_{in}) = [\mathcal{S}_1(Z_{in}), \mathcal{S}_2(Z_{in}), \cdots, \mathcal{S}_i(Z_{in})]^T$ and $\mathcal{S}_i(Z_{in})$ denote an activation function which is often chosen as Gaussian function.

$$\mathcal{S}_i(Z_{in}) = \exp\left[\frac{-\left(Z_{in} - u_i^T\right)\left(Z_{in} - u_i\right)}{\eta_i^2}\right], \quad i = 1, 2, \cdots, m, \tag{20}$$

where $u_i = [u_{i1}, u_{i2}, \cdots, u_{iq}]^T \in R^q$ is the center of receptive field and η_i is the variance.

From the definition of activation function, we can obtain that the $S(Z_{in})$ is bounded, which can be described as:

$$\|\mathcal{S}(Z_{in})\| \le \xi, \tag{21}$$

where ξ is a positive constant.

With a sufficiently large node m, any smooth continuous function can be approximated to any degree.

$$k_{nn}(Z_{in}) = W^{*T}\mathcal{S}(Z_{in}) + \varepsilon, \tag{22}$$

where W^* is the ideal weight over a compact set $\Omega_{Z_{in}} \subset R^q$. The approximation error of RBFNN satisfies $\|\varepsilon\| \le \rho$, where ρ is a small unknown constant.

Over a compact set $Z_{in} \in \Omega_{Z_{in}} \subset R^q$, the ideal weight vector can be represented as

$$W^* = \arg\min_{Z_{in} \in R}\left\{\sup\left|k_{nn}(Z_{in}) - W^T\mathcal{S}(Z_{in})\right|\right\}. \tag{23}$$

3.2. Model predictive tracking control

In this section, the model predictive tracking control is carried out with the RBFNN-based approximation. There are three key issues, including trajectory error function, system constraint and optimization objective function. The error equation is a mathematical description of the trajectory tracking control system. System constraints include controller constraints, control quantity constraints, and stability constraints. The objective function needs to consider the rapidity and smoothness of the trajectory tracking control.

According to (4), we can rewritten the kinematic model as

$$\begin{bmatrix} \dot{x} \\ \dot{y} \\ \dot{\varphi} \end{bmatrix} = \begin{bmatrix} \cos\varphi \\ \sin\varphi \\ \frac{2\tan\delta}{L(1+\tan\delta)} \end{bmatrix} v, \tag{24}$$

subjected to

$$\omega = \dot{\varphi} = \frac{v}{R} = \frac{2\tan\delta}{L(1+\tan\delta)} v, \tag{25}$$

where (x, y) is the center coordinate; φ is yaw angle, and v is the linear velocity of robot. In particular, according to the steering relationship of the wheel-legged robot [16], $R = \frac{L}{2} + \frac{L}{2\tan\delta}$.

Then the robot control system can be converted to input variable $u(v, \delta)$ and state variable $\chi(x, y, \varphi)$.

$$\chi = \mathcal{W}(x, u). \tag{26}$$

For the convenience of the MPC method design, we can define the expected motion trajectory as

$$\dot{\chi}_d = \mathcal{W}(\chi_d, u_d), \tag{27}$$

where expected state variable is $\chi_d = [x_d, y_d, \varphi_d]^T$ and expected input variable is $u_d = [v_d, \delta_d]$.

According to the Taylor theorem and ignoring the high-order values, (38) can be converted as

$$\begin{aligned} \dot{x} =& \mathcal{W}(x_d, u_d) + \left.\frac{\partial \mathcal{W}(x,u)}{\partial x}\right|_{x=x_d}(x - x_d) \\ &+ \left.\frac{\partial \mathcal{W}(x,u)}{\partial u}\right|_{x=x_d}(u - u_d). \end{aligned} \tag{28}$$

The error function can be represented as

$$\begin{aligned} x_e &= x(x) - x_d(x), \\ y_e &= y(x) - y_d(x), \\ \varphi_e &= \varphi(x) - \varphi_d(x). \end{aligned} \tag{29}$$

Thus, the path error function can be developed as

$$\begin{aligned} \dot{\chi}_e = \begin{bmatrix} \dot{x} - \dot{x}_d \\ \dot{y} - \dot{y}_d \\ \dot{\varphi} - \dot{\varphi}_d \end{bmatrix} &= \begin{bmatrix} 0 & 0 & -v_d\sin\varphi_d \\ 0 & 0 & v_d\cos\varphi_d \\ 0 & 0 & 0 \end{bmatrix} \chi_e \\ &+ \begin{bmatrix} \cos\varphi_d & 0 \\ \sin\varphi_d & 0 \\ \frac{2\tan\delta}{L(1+\tan\delta)} & \frac{2v_d}{L(1+\tan\varphi)^2\cos^2\delta_d} \end{bmatrix} u_e. \end{aligned} \tag{30}$$

In order to effectively implement tracking control, an improved objective function using relaxation factors can be represented as

$$\delta_d(k) = \sum_{i=1}^{N_P} \|\Upsilon(k+i|t) - \Upsilon_{\mathrm{ref}}(k+i|t)\|_{\mathcal{L}}^2$$

$$+\sum_{i=1}^{N_e-1}\|\Delta U(k+i|t)\|_{\mathcal{L}}^2+\sigma\psi^2, \tag{31}$$

where N_P is the prediction horizon; N_e is the control horizon; σ is the weight coefficient, and ψ is the weighting factor.

Note that the first term of the objective function reflects the ability of the robot system to track the reference trajectory, and the second term represents the capacity to constrain the control variable. This illustrates that the MPC controller can adequately realize the path tracking control, but cannot eliminate the uncertainties of the robot system and external interferences. However, the method of RBFNN approximation has shown the useful generalization [23, 24].

Then, we can transform the trajectory error model as

$$\phi(k|t)=[\widetilde{x}(k|t),\widetilde{u}(k-1|t)]^T. \tag{32}$$

The state function can be described as

$$\begin{aligned}&\phi(k+1|t)=\widetilde{\mathcal{H}}_{k,t}(k|t)+\widetilde{\mathcal{K}}_{k,t}\Delta U(k|t),\\&\Upsilon(k|t)=\tilde{Z}_{k,t}\phi(k|t),\end{aligned} \tag{33}$$

where $\widetilde{\mathcal{H}}_{k,t}=\begin{bmatrix}\mathcal{H}_{k,t} & \mathcal{K}_{k,t}\\ 0_{m\times n} & I_m\end{bmatrix}$, $\widetilde{\mathcal{K}}_{k,t}=[\mathcal{K}_{k,t},I_m]^T$, n is the state degree and m is the control variable degree.

Therefore, the output of model prediction can be obtained as follows:

$$Y_P(t)=\Theta_t\phi(t|t)+\mathrm{E}_t\Delta U(t|t). \tag{34}$$

Define the following vectors as

$$\begin{aligned}&H=I_m\otimes\begin{bmatrix}1&0&\cdots&\cdots&0\\1&1&0&\cdots&0\\1&1&1&\ddots&0\\\vdots&\vdots&\ddots&\ddots&0\\1&1&\cdots&1&1\end{bmatrix},\\&U_\lambda=1_{N_c}\otimes u(k-1),\end{aligned} \tag{35}$$

where 1_{N_c} is a column vector with the number of N_c; I_m is a unit matrix of order m and $\otimes$ is Kronecker product.

The optimization objective function can be represented as

$$\begin{aligned}&\mathcal{S}[\phi(t),u(t),\Delta U(t)]\\&=\mathcal{F}_t\left[\Delta U(t)^T,\psi\right]^T+\left[\Delta U(t)^T,\psi\right]^T\mathcal{D}_t\left[\Delta U(t)^T,\psi\right]^T,\end{aligned} \tag{36}$$

where $\mathcal{F}_t=\left[2e_t^T\mathcal{L}\mathcal{E}_t,0\right]$, $\mathcal{D}_t=\begin{bmatrix}\mathcal{E}_t^T\mathcal{L}\mathcal{E}_t+\mathcal{M} & 0\\ 0 & \sigma\end{bmatrix}$.

Therefore, the prediction horizon error can be obtained as

$$e_t=\Theta_t\phi(t|t)-Y_{\mathrm{ref}}(t), \tag{37}$$

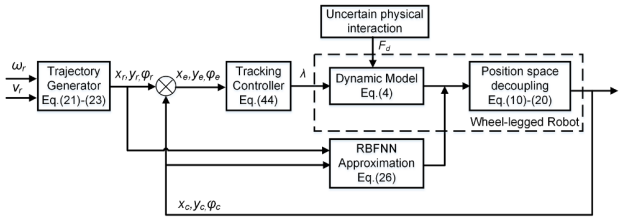

Fig. 2. Block diagram of RBFNN-based tracking control.

$$Y_{\mathrm{ref}}(t)=[\Upsilon_{\mathrm{ref}}(t+1|t),\cdots,\Upsilon_{\mathrm{ref}}(t+N_P|t)]^T. \tag{38}$$

When the model predictive controller completes the optimization objective function for each time, the control input increment of the system in the control horizon is defined as

$$\Delta U_t^*=\left[\Delta u_t^*,\Delta u_{t+1}^*,\cdots,\Delta u_{t+N_c-1}^*\right]^T. \tag{39}$$

Finally, substituting the first element of the control increment (67) into the control system as the actual control input increment

$$u(t)=u(t-1)+\Delta u_t^*. \tag{40}$$

Considering the safety and stability of the wheel-legged robot, it is necessary to restrict the control limit and control increment, as following:

$$u_{\min}(t+k)\le u(t+k)\le u_{\max}(t+k), \tag{41}$$

$$\Delta U_{\min}(t+k)\le\Delta U(t+k)\le\Delta U_{\max}(t+k), \tag{42}$$

where $k=1, 2, ..., t+N_c-1$.

3.3. Control block diagram

Based on the overall control scheme, the structure of RBFNN approximation for tracking control is shown in Fig. 2. The trajectory generator simulates the desired path and transfers the position information to the kinematics and dynamics model of the robot system. Then, the model predictive tracking controller is carried out to realize the path following in the undisturbed state according to the error of a lateral position, longitudinal position, and heading angle. For the model uncertainties and external disturbances, the RBFNN algorithm is applied to eliminate the uncertain physical interaction.

4. SYSTEM DESCRIPTION

Inspired by the Stewart parallel platform of the 6-degree-of-freedom (6-DOF) in the advantages of kinematics and dynamics, this paper developed the electric parallel wheel-legged robot (BIT-NAZA). It combines the rapidity and stability of wheel sport with strong adaptability of legged sport, making the robot movement more flexible and variable [25]. The developed concept of the

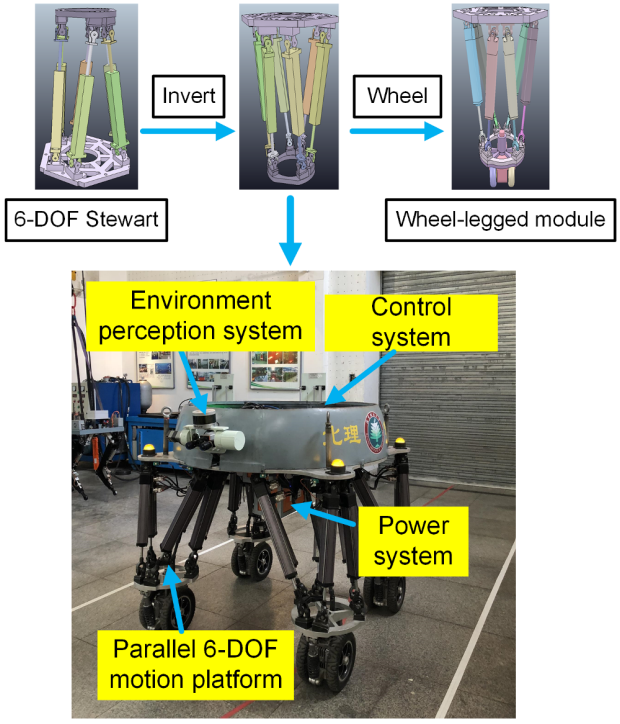

Fig. 3. Parallel mechanism of the wheel-legged robot.

Table 1. The main parameters of BIT-NAZA robot.

Size	1.2 m*1.2m*1.4m
Load capacity	150 kg (carrying)
Max wheel speed	15 km/h
Max legged Speed	1.2 m/s
The range of wheel track	0.5 m - 1 m
The range of base	1.2 m - 1.6 m

wheel-legged robot platform is shown in Fig. 3. The inverted Stewart parallel platform and drive wheel constitute a wheel-legged composite mechanism, which obtains a new sport model, including four-legged walking, four-wheel independent driving, and wheel-legged composite motion. The BIT-NAZA robot is mainly composed of the control system, environment perception system, power system, and parallel mechanical structure. In addition, the motion platform involves the electric cylinders, servo motors, suspension systems, and reducers. The corresponding parameters of the wheel-legged robot are shown in Table 1.

The communication network includes TCP/IP, CAN-bus, and RS232. The robot status information is transmitted to a monitor computer by wireless UDP transmission technology, and the cooperative control framework is implemented using the CAN bus. The robot device has been constructed using a DC motor and electric cylinder as the actuation element. The electric cylinder is GSM20-1202, with a 300 mm stroke, and the DC motor driver is Elmo.

Fig. 4. The motion sport of wheel-legged robot.

The energy system is a 48V20Ah power battery. The bottom controller adopts SCM/SGX1-PC104 module, and the central controller of the environmental perception system is TX2 (CPU: ARM+ Denver2; GPU: Pascal-GPU with 256 CUDA-cores).

There is a three-sport model in the wheel-legged robot, which is the wheel/foot model, the wheel-legged model, and the specific model, as shown in Fig. 4. When the obstacles are larger than the wheel track or higher than the base, the robot can autonomously switch to the wheel-legged sport. In practical application, the robot can transport 150 kg payload and cross the unstructured ground. Benefited by the various wheel-legged composite sport, the BIT-NAZA robot has the strong ability to walk in a complex environment such as military operations, emergency relief, resource exploration.

5. RESULTS AND DISCUSSIONS

In order to illustrate the effectiveness of the proposed algorithms, some demonstrations are carried out on the developed electric parallel wheel-legged robot (BIT-NAZA). Two groups of comparative test are carried out as follows:

- Trajectory tracking without external disturbances of PID and NMPC, including straight lines, curves and obstacles, is designed to verify the accuracy and robustness of the proposed algorithm.

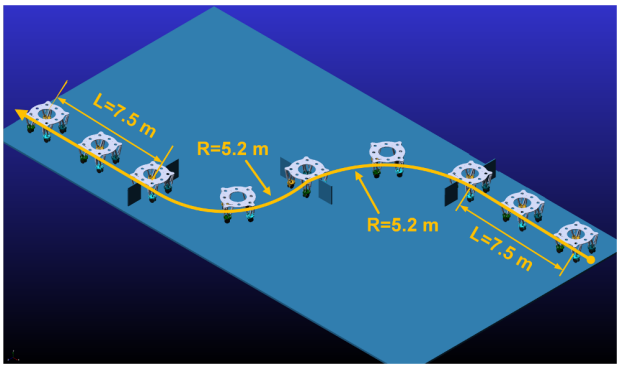

Fig. 5. The tracking performance of S-shape.

- In contrast, to further explain the advantage of NMPC in uncertain disturbances, including the internal-robot friction and external-robot and environment interaction forces, a comparison using NMPC and MPC is discussed for the circle path.

The main experiment parameter setting are as follows: robot speed $v = 1$ m/s, prediction horizon $N_P = 20$, control horizon $N_e = 5$, weight coefficient $\sigma = 10$, MPC sample time $T = 0.02$ s, interference signal of sine curve $d = 0.015$ and period $t = 2$ s. In order to control the ability of stability and smoothness, we define the constraint condition of the control variable as $[-0.3, -25]^T \leq u \leq [0.3, 25]^T$ and $[-0.02, -0.05]^T \leq \Delta U \leq [0.02, 0.05]^T$. At the same time, the weight matrix of RBFNN are initialized as $W_1(0) = \mathbf{0} \in \mathbb{R}^{3l_1 \times 3}$ and $W_2(0) = \mathbf{0} \in \mathbb{R}^{3l_2 \times 3}$, and the momentum parameter and the learning rate of RBFNN are set as 0.00005 and 0.000005, respectively. $\eta_i = 1.1$ and $u_i = \begin{bmatrix} -3 & -1.5 & 0 & 1.5 & 3 & 3.5 \end{bmatrix}$.

In Fig. 5, the target path is mainly composed of the straight path with 7.5 meters, the circular arc with a radius of 5.2 meters and three obstacles with narrow aisles. The width of the barrier is only 4cm more extensive than the robot body to verify the accuracy of the control algorithm. Set the robot to advance at a uniform speed of 1 m/s, and pass the trajectory of straight, arcs and obstacles in sequence. The comparative results of co-simulation are displayed in Fig. 6. It can be seen from the co-simulation results that the proposed algorithm NMPC can track the reference path well, and the robot responds smoothly with a lateral error of around ± 0.05 meters. Both the lateral position and the longitudinal position are capable of tracking the reference path, whether in straight sections or curve sections. However, the wheel-legged robot using the PID scheme has a large fluctuation in tracking trajectory with the lateral error around ± 0.1 meters and heading angle error around 4 degrees. The control response of accuracy and frequency does not meet the fast real-time in the robot system. In addition, the NMPC can accurately pass through the uncertain disturbances of narrow aisles (8s, 15s, and 23s), while the robot with PID approach collided when passing the second obstacle, indicating that the NMPC algorithm can achieve satisfactory performance with high accuracy and respond quickly in tracking performances.

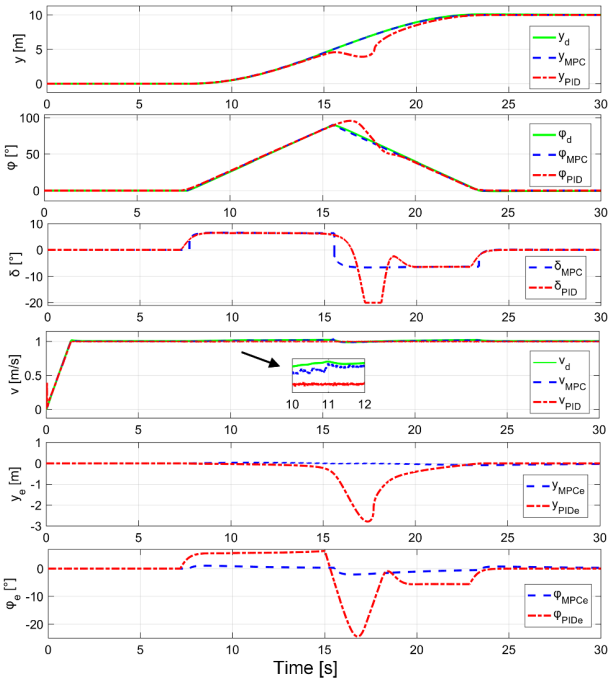

Fig. 6. The comparative results of PID and MPC.

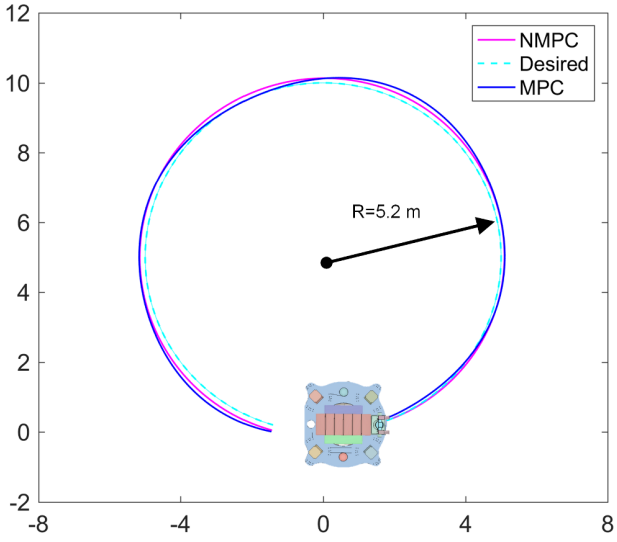

Fig. 7. The tracking performance of tracking control with NMPC and MPC.

To further evaluate the superiority and universality of the proposed algorithm, a circular path with 5.2 meters tracking experiment using NMPC and MPC under uncertain physical interaction with sinusoid input is investigated, and the tracking performance is displayed in Fig. 7. There are the comparative results of longitudinal position,

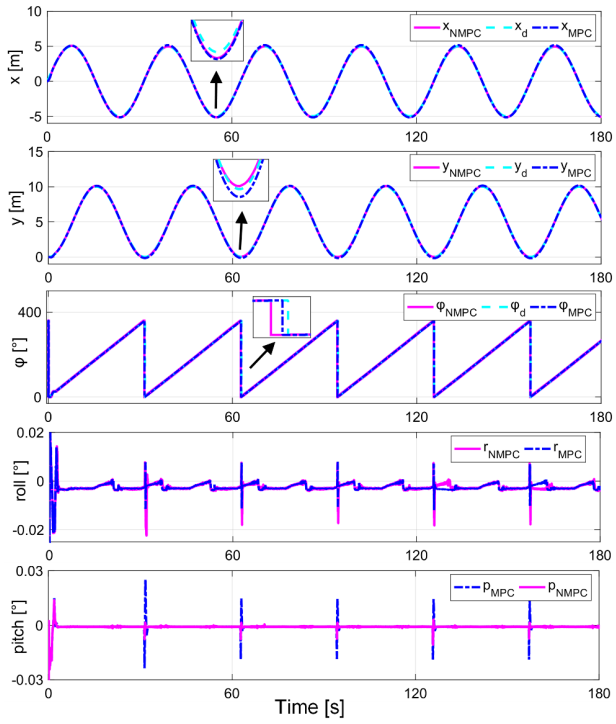

Fig. 8. The comparative performances of NMPC and MPC in longitudinal position, lateral position, heading angle, roll angle and pitch angle.

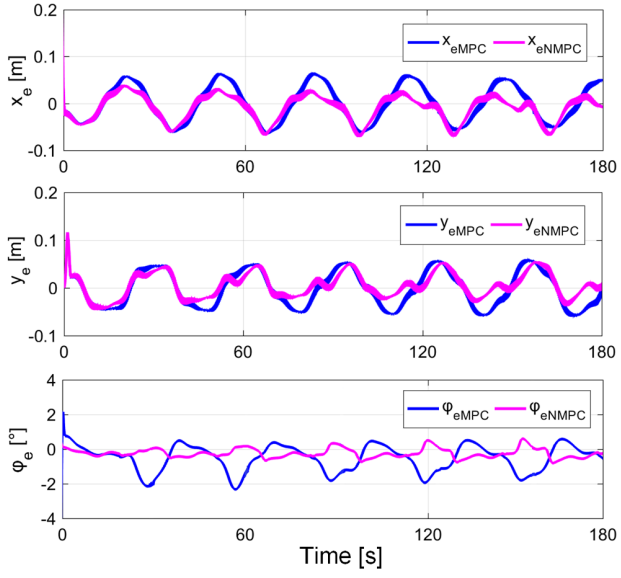

Fig. 9. The tracking error of NMPC and MPC in longitudinal position, lateral position and heading angle.

lateral position, heading angle, roll angle and pitch angle, as noted in Fig. 8. It can be seen that both the NMPC and MPC approach can basically track the desired trajectory. However, from the tracking error of NMPC and MPC, as presented in Fig. 9, the system with NMPC can be controlled to track the desired trajectory with the gradually decreasing error variation in the lateral position, longitudinal position and heading angle, while the tracking error of the MPC scheme is slowly increasing. The lateral error of NMPC is efficiently controlled within ± 0.02 meters, which means that in the case of external interference and uncertain dynamics, the NMPC can obtain the higher control accurately, and the tracking error is gradually reduced. In addition, the method of NMPC can maintain a smaller pitch angle and roll angle, which means that the NMPC can achieve the advantage of performance in the case of uncertain dynamics.

Based on the obtain tracking performance, we can infer that the RBFNN approximation can be properly compensated for the internal interference and external uncertainty of the robot system. The proposed algorithm NMPC has higher position control accuracy than the classical MPC, especially in more precise and smoother in lateral error.

6. CONCLUSION

This paper investigates the neural approximation-based model predictive tracking control for the developed wheel-legged robot under the uncertain physical interaction and external dynamics. The proposed NMPC approach can adequately compensate for dynamic uncertainties. In addition, an advanced parallel mechanism of wheel-legged is introduced to validate the proposed algorithm. Some demonstrations are performed using the BIT-NAZA robot to illustrate that the proposed method can achieve promising tracking performance, which can provide theoretical and engineering guidance for intelligent robots. To improve our future research, we will endeavor to consider the dynamic analysis of impedance control and more complicated road conditions in a practical robot system.

REFERENCES

[1] N. T. Binh, N. A. Tung, D. P. Nam, and N. H. Quang, "An adaptive backstepping trajectory tracking control of a tractor trailer wheeled mobile robot," *International Journal of Control, Automation and Systems*, vol. 17, pp. 465-473, 2019.

[2] Y. Zhao, Y. Zhang, and J. Lee, "Lyapunov and sliding mode based leader-follower formation control for multiple mobile robots with an augmented distance-angle strategy," *International Journal of Control, Automation and Systems*, vol. 17, no. 17, pp. 1-8, 2019.

[3] X. Zhang, J. Li, Z. Hu, W. Qi, L. Zhang, Y. Hu, H. Su, G. Ferrigno, and E. D. Momi, "Novel design and lateral stability tracking control of a four-wheeled rollator," *Applied Sciences*, vol. 9, no. 11, 2327, 2019.

[4] F. Michaud, D. Letourneau, M. Arsenault, Y. Bergeron, R. Cadrin, F. Gagnon, M.-A. Legault, M. Millette, J.-F. Paré, M.-C. Tremblay, P. Lepage, Y. Morin, J. Bisson, and S. Caron, "Multi-modal locomotion robotic platform

using leg-track-wheel articulations," *Autonomous Robots*, vol. 18, no. 2, pp. 137-156, 2005.

[5] D.-Y. Lee, G.-P. Jung, M.-K. Sin, S.-H. Ahn, and K.-J. Cho, "Deformable wheel robot based on origami structure," *Proc. of IEEE International Conference on Robotics and Automation*, pp. 5612-5617, 2013.

[6] D. Lu, E. Dong, C. Liu, M. Xu, and J. Yang, "Design and development of a leg-wheel hybrid robot "HyTRo-I"," *Proc. of IEEE/RSJ International Conference on Intelligent Robots and Systems*, pp. 6031-6036, 2013.

[7] Z. Li, J. Deng, R. Lu, X. Yong, and C. Y. Su, "Trajectory-tracking control of mobile robot systems incorporating neural-dynamic optimized model predictive approach," *IEEE Transactions on Systems Man & Cybernetics Systems*, vol. 46, no. 6, pp. 740-749, 2017.

[8] H. Peng, J. Wang, S. Wang, W. Shen, D. Shi, and D. Liu, "Coordinated motion control for a wheel-leg robot with speed consensus strategy," *IEEE/ASME Transactions on Mechatronics*, vol. 25, no. 3, pp. 1366-1376, 2020.

[9] Z. Shuai, H. Zhang, J. Wang, J. Li, and M. Ouyang, "Combined AFS and DYC control of four-wheel-independent-drive electric vehicles over can network with time-varying delays," *IEEE Transactions on Vehicular Technology*, vol. 63, no. 2, pp. 591-602, 2013.

[10] D. Xu, Y. Shi, and Z. Ji, "Model-free adaptive discrete-time integral sliding-mode-constrained-control for autonomous 4WMV parking systems," *IEEE Transactions on Industrial Electronics*, vol. 65, no. 1, pp. 834-843, 2017.

[11] R. Cui, L. Chen, C. Yang, and M. Chen, "Extended state observer-based integral sliding mode control for an underwater robot with unknown disturbances and uncertain nonlinearities," *IEEE Transactions on Industrial Electronics*, vol. 64, no. 8, pp. 6785-6795, 2017.

[12] Z. Li, C. Yang, C.-Y. Su, J. Deng, and W. Zhang, "Vision-based model predictive control for steering of a nonholonomic mobile robot," *IEEE Transactions on Control Systems Technology*, vol. 24, no. 2, pp. 553-564, 2015.

[13] H. Su, W. Qi, C. Yang, A. Aliverti, G. Ferrigno, and E. Momi, "Deep neural network approach in human-like redundancy optimization for anthropomorphic manipulators," *IEEE Access*, vol. 7, pp. 124207-124216, 2019.

[14] H. Su, W. Qi, Y. Hu, J. Sandoval, L. Zhang, Y. Schmirander, G. Chen, A. Aliverti, A. Knoll, G. Ferrigno, and E. de Momi, "Towards model-free tool dynamic identification and calibration using multi-layer neural network," *Sensors*, vol. 19, no. 17, p. 3636, 2019.

[15] H. Su, C. Yang, H. Mdeihly, A. Rizzo, G. Ferrigno, and E. De Momi, "Neural network enhanced robot tool identification and calibration for bilateral teleoperation," *IEEE Access*, vol. 7, pp. 122041-122051, 2019.

[16] J. Li, J. Wang, S. Wang, H. Peng, B. Wang, W. Qi, L. Zhang, and H. Su, "Parallel structure of six wheel-legged robot trajectory tracking control with heavy payload under uncertain physical interaction," *Assembly Automation*, 2020.

[17] Z. Li, S. Xiao, S. S. Ge, and H. Su, "Constrained multilegged robot system modeling and fuzzy control with uncertain kinematics and dynamics incorporating foot force optimization," *IEEE Transactions on Systems, Man, and Cybernetics: Systems*, vol. 46, no. 1, pp. 1-15, 2015.

[18] Y. Hu, H. Su, L. Zhang, S. Miao, G. Chen, and A. Knoll, "Nonlinear model predictive control for mobile robot using varying-parameter convergent differential neural network," *Robotics*, vol. 8, no. 3, p. 64, 2019.

[19] H. Su, W. Qi, C. Yang, J. Sandoval, G. Ferrigno, and E. Momi, "Deep neural network approach in robot tool dynamics identification for bilateral teleoperation," *IEEE Robotics and Automation Letters*, vol. 5, no. 2, pp. 2943-2949, 2020.

[20] W. Qi, H. Su, C. Yang, G. Ferrigno, E. Momi, and A. Aliverti, "A fast and robust deep convolutional neural networks for complex human activity recognition using smartphone," *Sensors*, vol. 19, no. 17, 3731, 2019.

[21] F. Ke, Z. Li, and C. Yang, "Robust tube-based predictive control for visual servoing of constrained differential-drive mobile robots," *IEEE Transactions on Industrial Electronics*, vol. 65, no. 4, pp. 3437-3446, 2017.

[22] H. Su, J. Sandoval, M. Makhdoomi, G. Ferrigno, and E. Momi, "Safety-enhanced human-robot interaction control of redundant robot for teleoperated minimally invasive surgery," *Proc. of IEEE International Conference on Robotics and Automation (ICRA)*, pp. 6611-6616, IEEE, 2018.

[23] H. Su, J. Sandoval, P. Vieyres, G. Poisson, G. Ferrigno, and E. Momi, "Safety-enhanced collaborative framework for tele-operated minimally invasive surgery using a 7-DoF torque-controlled robot," *International Journal of Control, Automation and Systems*, vol. 16, no. 6, pp. 2915-2923, 2018.

[24] H. Su, S. Ertug Ovur, Z. Li, Y. Hu, J. Li, K. Alois, G. Ferrigno, and E. Momi, "Internet of things (IoT)-based collaborative control of a redundant manipulator for teleoperated minimally invasive surgeries," in *2020 International Conference on Robotics and Automation (ICRA)*, IEEE, 2020.

[25] H. Peng, J. Wang, W. Shen, and D. Shi, "Cooperative attitude control for a wheel-legged robot," *Peer-to-Peer Networking and Applications*, no. 3, pp. 1-12, 2019.

Jiehao Li received his M.Sc. degree in control engineering from South China University of Technology, Guangzhou, China, in 2017. He is pursuing a Ph.D. degree as a member of State Key Laboratory of Intelligent Control and Decision of Complex Systems, Beijing Institute of Technology, China, and as a visiting research fellow of the Medical and Robotic Surgery Group (NEARLab) and the Department of Electronics, Information and Bioengineering (DEIB) in Politecnico di Milano, Milan, Italy, where he is working on the intelligent control and practical application for mobile robots.

Junzheng Wang received his Ph.D. degree in control science and engineering from Beijing Institute of Technology, Beijing, China, in 1994. He is the Deputy Director with the Key Laboratory of Intelligent Control and Decision of Complex Systems, Beijing Institute of Technology, where he is a Professor and a Ph.D. Supervisor. His current research interests include motion control, static and dynamic performance testing of electric and electric hydraulic servo system, and dynamic target detection and tracking based on image technology. Prof. Wang is a senior member of the Chinese Mechanical Engineering Society and the Chinese Society for Measurement. He received the Second Award from the National Scientific and Technological Progress (No.1) in 2011.

Shoukun Wang received his B.S., M.S., and Ph.D. degree in the department of automation, from Beijing Institute of Technology, Beijing, China, in 1999, 2002, and 2004, respectively. He has entered in the Department of Electronics and Computer Engineering, Purdue University, West Lafayette, USA, as a visiting scholar. He has been teaching at the School of Automation, Beijing Institute of Technology, since 2004. His research interests include sensor, measurement, and electro-hydraulic control. He has participated in over 30 scientific research projects since 2001, which mainly belong to measurement and servo control. He has also served as the leader in some of these works. His main work focused on electrical-hydraulic control algorithm, robot locomotion control, and visual systems.

Wen Qi received her M.Sc. degree in control engineering from the South China University of Technology, Guangzhou, China, in 2015. Her first-authored paper was awarded the finalist of T J Tarn's Best Paper Award on Control Applications on IEEE WCICA 2014. Now she is pursuing a Ph.D. degree as a member of the Laboratory of Biomedical Technologies (TBMLab) in Politecnico di Milano, Milano, Italy. Her main research interests include machine learning, deep learning and signal processing algorithms in wearable medical devices.

Longbin Zhang received her M.S degree in control engineering from South China University of Technology, Guangzhou, China, in 2017. She is currently pursuing a Ph.D. degree in Department of Mechanics, KTH Royal Institute of Technology, Stockholm, Sweden, working on robotic exoskeletons for patients with motor disorders. Her main research interests include human movement simulation, strategies, consequences, and assistance in patients with motor disorders, and adaptive control.

Yingbai Hu received his M.Sc. degree in control theory and control engineering from South China University of Technology, Guangzhou, China, in 2017. He is currently working toward a Ph.D. degree in computer science as a member of the Informatics 6-Chair of Robotics, Artificial Intelligence and Real-time Systems in Technische Universität München, München, Germany. His main research interests include control and instrumentation in mobile robot, human-robot interaction, surgical robotics, reinforcement learning, etc.

Hang Su received his M.Sc. degree in control theory and control engineering from South China University of Technology, Guangzhou, China, in 2015. He obtained his Ph.D. degree in 2019 as a member of the Medical and Robotic Surgery group (NEARLab) in Politecnico di Milano, Milano, Italy. He participated in the EU funded project (SMARTsurg) in the field of Surgical Robotics. Dr. Hang Su is currently a Research Fellow in the Department of Electronics, Information and Bioengineering (DEIB) of Politecnico Di Milano. He is fostering an international research team constituting three PhD students and a few Masters students in the field of Medical Robotics. He serves as an Associate Editor for IEEE International Conference on Robotics and Automation (ICRA) and IEEE/RSJ International Conference on Intelligent Robots and Systems (IROS). He also has served as a reviewer for over 30 scientific journals, such as IEEE Transaction on Biomedical Engineering, IEEE/ASME Transactions on Mechatronics, IEEE Transaction on Automation and Engineering, IEEE Transaction on Cybernetics, IEEE Transactions on Systems, Man, and Cybernetics: Systems, etc.. He is currently Special Session Chair of IEEE International Conference on Advanced Robotics and Mechatronics (ICARM 2020). He has published several papers in international conferences and journals and has been awarded ICRA 2019 travel grant. His main research interests include control and instrumentation in medical robotics, human-robot interaction, surgical robotics, deep learning, bilateral teleoperation, etc.